



# N-Linked glycan site occupancy impacts the distribution of a potassium channel in the cell body and outgrowths of neuronal-derived cells



M.K. Hall, D.A. Weidner, C.J. Bernetski, R.A. Schwalbe \*

Department of Biochemistry and Molecular Biology, Brody School of Medicine at East Carolina University, Greenville, NC 27834, USA

## ARTICLE INFO

### Article history:

Received 20 June 2013

Received in revised form 30 September 2013

Accepted 16 October 2013

Available online 23 October 2013

### Keywords:

N-glycosylation

Potassium channel

Membrane glycoprotein

Membrane trafficking

High density potassium channel cluster

Excitable membrane

## ABSTRACT

**Background:** Vacancy of occupied N-glycosylation sites of glycoproteins is quite disruptive to a multicellular organism, as underlined by congenital disorders of glycosylation. Since a neuronal component is typically associated with this disease, we evaluated the impact of N-glycosylation processing of a neuronal voltage gated potassium channel, Kv3.1b, expressed in a neuronal-derived cell line, B35 neuroblastoma cells.

**Methods:** Total internal reflection fluorescence and differential interference contrast microscopy measurements of live B35 cells expressing wild type and glycosylation mutant Kv3.1b proteins were used to evaluate the distribution of the various forms of the Kv3.1b protein in the cell body and outgrowths. Cell adhesion assays were also employed. **Results:** Microscopy images revealed that occupancy of both N-glycosylation sites of Kv3.1b had relatively similar amounts of Kv3.1b in the outgrowth and cell body while vacancy of one or both sites led to increased accumulation of Kv3.1b in the cell body. Further both the fully glycosylated and partially glycosylated N229Q Kv3.1b proteins formed higher density particles in outgrowths compared to cell body. Cellular assays demonstrated that the distinct spatial arrangements altered cell adhesion properties.

**Conclusions:** Our findings provide direct evidence that occupancy of the N-glycosylation sites of Kv3.1b contributes significantly to its lateral heterogeneity in membranes of neuronal-derived cells, and in turn alters cellular properties.

**General significance:** Our study demonstrates that N-glycans of Kv3.1b contain information regarding the association, clustering, and distribution of Kv3.1b in the cell membrane, and furthermore that decreased occupancy caused by congenital disorders of glycosylation may alter the biological activity of Kv3.1b.

© 2013 Elsevier B.V. All rights reserved.

## 1. Introduction

N-Glycosylation to newly synthesized membrane proteins is the most abundant protein co-translational modification in the lumen of the endoplasmic reticulum [1]. N-Linked oligosaccharides have been shown to be involved in protein folding, protein assembly, and intracellular protein sorting while outside the cell they are engaged in cell recognition events [2]. For instance, the presence of N-glycans attached to apical membrane proteins are critical for their trafficking to and retention in the apical membranes [3]. It has also been shown that the number of complex N-glycans and the degree of N-glycan branching increase expression of cell surface glycoproteins [4]. Since the majority of membrane proteins is N-glycosylated, and a vital property conveyed by

integral membrane proteins is their lateral heterogeneity in biological membranes, it is of considerable importance to understand the impact that the number and position of N-glycans have on the spatial arrangement of membrane proteins in plasma membranes. This would further reinforce the role of glycans as informational biopolymers.

Voltage-gated potassium channels (Kv) are critical components in the generation and propagation of electrical excitability in the nervous system [5]. A less defined role of Kv channels is their non-conducting functions, such as cell–cell interactions, cell migration, and cell proliferation [6]. The Kv3 channel subfamily members, Kv3.1–Kv3.4, have two absolutely conserved N-glycosylation sites within their S1–S2 extracytoplasmic linkers. Both of the two N-glycosylation sites of Kv3.1 [7], Kv3.3, and Kv3.4 are occupied throughout the rat central nervous system [8]. There are two different carboxyl-terminus Kv3.1 splice variants (Kv3.1a, and b) with Kv3.1b as the more abundant variant [9]. Kv3.1 splice variants are localized to the axonal and somatodendritic compartments of neurons but at significantly different levels [10]. When either one or both of the N-glycosylation sites of the Kv3.1b channel were vacated, the heterologously expressed ionic currents have decreased activation, inactivation and deactivation rates, as well

**Abbreviations:** Kv channel, voltage-gating potassium channel; CB, cell body; OG, outgrowth; CDG, congenital disorder of glycosylation; TIRF, total internal reflection fluorescence; DIC, differential interference contrast; Neu, neuraminidase

\* Corresponding author at: Department of Biochemistry and Molecular Biology, Brody School of Medicine at East Carolina University, 600 Moye Boulevard, Greenville, NC 27834, USA. Tel.: +1 252 744 2034; fax: +1 252 744 3383.

E-mail address: [schwalber@ecu.edu](mailto:schwalber@ecu.edu) (R.A. Schwalbe).

as reduced cell migratory rates [11]. Additionally, partial substitution of the natural sialic acids with non-natural sialic acids of the *N*-glycans of Kv3.1b glycoprotein generated decreased activation and inactivation rates of the outward ionic currents [12]. Other Kv channels which lack *N*-glycosylation occupancy, as well as sialic acid residues, have also been shown to have altered channel gating [13]. The importance of *N*-glycosylation site occupancy of glycoproteins is emphasized by congenital disorders of glycosylation (CDG) [14]. Further dysfunction and expression levels of Kv3 channels have been linked to other diseases of the nervous system [15], as well as colon cancer [16]. Therefore, the modulation of the conducting and non-conducting functions of the Kv3.1b channel is of importance in health and disease.

Since CDG reveals that the vacancy of naturally occupied *N*-glycosylation sites of glycoproteins is disruptive to human neurology, the present investigation was undertaken to examine whether the number and position of *N*-glycans attached to the Kv3.1b protein influence the distribution of the Kv3.1b protein to the outgrowths and cell body of B35 neuroblastoma cells, and furthermore address whether these different spatial arrangements correlate to changes in the conducting and non-conducting functions of the Kv3.1b channel. We selected B35 neuroblastoma cells, a cultured neuronal-derived cell model, since they are commonly employed to investigate neurites and cell motility [17]. Total internal reflection fluorescence (TIRF) and differential interference contrast (DIC) microscopy measurements were performed to evaluate the distribution of the various forms of the glycosylated Kv3.1b protein, as well as the unglycosylated Kv3.1b protein, in live B35 cells. Cell dissociation and association assays were conducted to assess the strength of cell–cell interactions and size of cell aggregates. We observed that vacancy of one or both *N*-glycosylation sites of the Kv3.1b protein decreases the amount of the Kv3.1b protein in the outgrowth relative to the cell body of neuronal-derived cells which correlated with decreases in cell migration [11] and cell–cell adhesiveness. Additionally, the formation of high density particles in the neuronal outgrowths was observed for the fully glycosylated and partially glycosylated N229Q Kv3.1b proteins, unlike the unglycosylated and partially glycosylated N220Q Kv3.1b proteins. Based on the present study, along with our previous study [11], the formation of these high density clusters correlated with more noninactivating whole cell current patterns than inactivating whole cell current patterns for cells expressing the Kv3.1b channel.

## 2. Materials and methods

### 2.1. Molecular biology

Polymerase chain reaction (PCR) was employed to fuse EGFP to the C-termini of wild type and glycosylation mutant Kv3.1b cDNAs [11]. We used *Rattus rattus* Kv3.1b cDNA (accession no. P25122). Briefly, the stop sites and BamHI sites were added to the 5' and 3' ends of wild type, N220Q/N229Q, N220Q, and N229Q Kv3.1b cDNAs in pCDNA3.1 vectors. These cDNAs were sequenced, digested with BamHI (New England BioLabs, Ipswich, MA, USA) and then inserts were isolated. Subsequently, each of the inserts was fused into a digested BamHI pEGFP-N3 vector (Clontech, Mountain View, CA, USA) to generate Kv3.1b-pEGFP-N3, N220Q/N229Q-pEGFP-N3, N220Q-pEGFP-N3, and N229Q-pEGFP-N3 recombinant vectors. Orientations in the recombinant vectors were verified using SmaI (New England BioLabs, Ipswich, MA, USA) digests. Standard procedures were followed for DNA amplification, DNA isolation, and subcloning [11].

### 2.2. B35 neuroblastoma cell culture and the establishment of stable cell lines

B35 neuroblastoma cells (rat central nervous system, derived) were obtained from the American Type Culture Collection (Manassas, VA, USA) and maintained in DMEM (Mediatech Inc., Manassas, VA, USA)

supplemented with 10% fetal bovine serum (Invitrogen, Carlsbad, CA, USA), penicillin (50 U/mL) (Invitrogen, Carlsbad, CA, USA), and streptomycin (50 µg/mL) (Invitrogen, Carlsbad, CA, USA) at 37 °C under 5% CO<sub>2</sub> (ref). B35 cells were plated on uncoated 60 mm dishes (Fisher Scientific, Suwanee, GA, USA) every 3–4 days after a brief trypsin-EDTA (Invitrogen, Carlsbad, CA, USA) treatment and the cell culture medium was changed every 2–3 days. For the production of stable cell lines expressing the various forms of the Kv3.1 protein, B35 cells of 75–80% confluency were transfected with neomycin selectable pEGFN3 expression plasmids encoding wild type, N200Q/N229Q, N220Q, and N229Q Kv3.1b proteins using Lipofectamine™ 2000 (Invitrogen, Carlsbad, CA, USA) according to the manufacturer's protocol. In brief, FBS and antibiotic free B35 cell culture media (1 mL) containing about 8 µg of recombinant vector and 15 µL of Lipofectamine™ 2000 (Invitrogen, Carlsbad, CA, USA) were added to each dish. Following an incubation of 5 h with the DMEM–DNA–lipid transfection solution, each dish of the B35 cells was re-fed with 3 mL of serum and antibiotic containing DMEM medium. B35 cells were selected for stable transfectants by the addition of 1.0 g/L of Geneticin® (Invitrogen, Carlsbad, CA, USA) to the cell culture medium. After this treatment, B35 cells expressing the various Kv3.1b-EGFP proteins were further enriched using a FACS Vantage (Becton Dickinson, Franklin Lakes, NJ, USA) cell sorter with laser excitation at 488 nm and green fluorescence emission at 515–545 nm. Isolated stable pools of transfected cells were then used for subsequent studies.

### 2.3. B35 total membrane isolation

B35 cells expressing wild type, N220Q/N229Q, N220Q, and N229Q Kv3.1b EGFP fusion proteins (about  $1.35 \times 10^8$ ) were homogenized (30–50 strokes) in 3 mL of lysis buffer (10 mM Tris (pH 7.4)); 250 mM sucrose, 5 mM EDTA; protease inhibitor cocktail set III 1:500 (Calbiochem, San Diego, USA), and subsequently centrifuged at 2000 ×g in an Eppendorf F-45-30-11 rotor (Eppendorf, Westbury, NY, USA) for 10 min at 4 °C. The supernatant was then centrifuged at 100,000 ×g in an AH650 rotor (Sorvall, Newtown, CT, USA) for 1 h at 4 °C. The high speed pellet was resuspended in about 200 µL lysis buffer and the protein concentration was determined by the method of Lowry. Samples were then stored at –80 °C until needed.

### 2.4. Glycosidase digestions of total B35 membranes

Total B35 membranes (5 g/L) containing wild type, N220Q/N229Q, N220Q and N229Q Kv3.1 proteins fused to EGFP were treated with PNGase F (20 U/µL) (New England Biolabs, Ipswich, MA, USA), Endo H (50 U/µL) (New England Biolabs, Ipswich, MA, USA), or neuraminidase (0.83 U/µL) (New England Biolabs, Ipswich, MA, USA) in buffers supplied by NEB. Reactions were allowed to proceed overnight at 37 °C. Reactions were stopped by addition of reducing SDS–PAGE sample buffer (2×).

### 2.5. Immunoblotting

For preparation of immunoblots, reducing SDS sample buffer (2×) was added to B35 membranes, and was subjected to electrophoresis for 105 min at 20 mA on 10% SDS gels. Electrophoresed proteins were transferred to Immobilon-P PVDF membranes (Millipore, Billerica, MA, USA) for 240 min at 250 mA. Blots were then incubated at room temperature for 20 min in blocking buffer (PBS, 3% BSA with 0.1% Tween 20) followed by incubation for 2 h in polyclonal rabbit anti-Kv3.1 antibody (Alomone Labs, Jerusalem, Israel). The specificity of the anti-Kv3.1 antibody has been previously described [7]. Subsequently blots were washed, and then incubated overnight at 4 °C with anti-rabbit antibody conjugated to alkaline phosphatase. Finally, immunobands were developed with immunoalkaline phosphatase substrate (MP Biomedicals, Irvine, CA, USA).

## 2.6. TIRF microscopy

Stable transfected B35 cells expressing wild type Kv3.1b-EGFP, N220Q/N229Q-EGFP, N220Q-EGFP, and N229Q-EGFP were seeded onto 35 mm ploy-L-lysine coated glass bottom dishes (MatTek, Ashland, Ma, USA) and kept under culturing conditions for about 15–18 h before imaging. Images were excited with an argon laser beam of wavelength 488 nm entering the side illumination port of an Olympus 1×-71 microscope through an Apo 60×1.45 objective and an ORCA R2 deep cooled mono CCD camera. Detection settings were kept constant for comparisons of the glycosylated, unglycosylated and partially glycosylated Kv3.1 proteins. The shutters, filters and camera, as well as data acquisition were controlled by Cell<sup>^</sup>TIRF Control 1.1 and MetaMorph for Olympus Basic software. Exposure time of 1000 ms was utilized for data analysis. Image J software was used for mean data analysis. Origin 7.5 was used for graphics and statistics. Data is presented as the mean  $\pm$  S.E. where  $n$  denotes the number of cells tested. Student's  $t$ -test was employed to evaluate the statistical comparison. Statistical significance was considered at  $P < 0.05$ .

## 2.7. Dissociation assays

Stable transfected B35 cells expressing wild type Kv3.1b-EGFP and N220Q/N229Q-EGFP and nontransfected cells were seeded in equal concentrations and allowed to grow for 2 days on 60 mm CellBind culture dishes (Corning, Corning, NY, USA). Confluent dishes were washed twice with PBS and resuspended in DMEM. Cells were detached by one complete rotation with a cell scraper and then cell aggregates were dissociated by pipetting ten times. Images (30–35 fields/dish) were obtained on an Olympus IX 50 microscope using a 20× objective. Particles ( $\geq 2$  cells/aggregate) were counted, and their areas determined using Image J software. Data is presented as the mean  $\pm$  S.E. where  $n$  denotes the number of particles. Student's  $t$ -test was used to evaluate the statistical comparison. Statistical significance was considered at  $P < 0.05$ .

## 2.8. Classical cell aggregation assay

B35 neuroblastoma cells were treated with PBS/10 mM EDTA for 5 min at room temperature and dispersed by pipetting. After two washes with Hanks Balanced Salt Solution the cells ( $10^5$  cells/mL) were resuspended in Hanks Balanced Salt Solution with either 1 mM  $\text{CaCl}_2$  or 5 mM EDTA and seeded into 12 well plates (Thermo Fisher Scientific, Atlanta, GA, USA) pre-coated with 2% BSA (Sigma, St. Louis, MO, USA). Plates were placed on a rotating, gyrating platform at 37° for 40 min. Aggregation reactions were stopped by adding 8% glutaraldehyde (Sigma, St. Louis, MO, USA). Images (6 fields/well) were taken with an Olympus IX50 (Olympus, Center Valley, PA) microscope using 10× objective. Areas of particles ( $> 10$  cells per aggregate) were determined using Image J software. Data is presented as the mean  $\pm$  S.E. where  $n$  denotes the number of images. Student's  $t$ -test was used to evaluate the statistical comparison. Statistical significance was considered at  $P < 0.01$ .

## 2.9. Hanging drop aggregation assay

B35 neuroblastoma cells were treated with 0.5% trypsin and 0.5 mM EDTA for 5 min at room temperature. Cells were washed 2× in PBS and resuspended in DMEM (Mediatech) at a concentration of  $5.0 \times 10^5$  cells/mL. Drops (30  $\mu\text{L}$ ) of cell suspension containing about  $1.5 \times 10^4$  cells/drop were placed on the inner surface of the lid of a 24 well cell culture dish and the lid was inverted over the culture wells which contained 0.5 mL of PBS to prevent evaporation of the hanging drop. The cells were cultured overnight in the hanging drop at 37°. The lids were inverted and the weak aggregates were disrupted by pipetting up and down 7 times using a standard 200  $\mu\text{L}$  pipet tip. Images (3 fields/well) were taken with an Olympus IX50 microscope (Olympus, Center Valley, PA) using

10× and 40× objectives. Image J software was utilized to ascertain area of particles ( $> 10$  cells per aggregate). Data is presented as the mean  $\pm$  S.E. where  $n$  denotes the number of particles. Student's  $t$ -test was used to evaluate the statistical comparison. Statistical significance was considered at  $P < 0.05$ .

## 3. Results

### 3.1. Characterization of the various forms of the Kv3.1b protein

Previously, glycosylated (wild type), unglycosylated (N220Q/N229Q), and partially glycosylated (N220Q and N229Q) Kv3.1b proteins were expressed in B35 neuroblastoma cells to show that  $N$ -glycan occupancy of the Kv3.1b glycoprotein could influence outward ionic current kinetics [11]. Here we have utilized this same expression system to ascertain whether  $N$ -glycosylation occupancy of the Kv3.1b protein could affect the number and size of Kv3.1b particles in the cell body and outgrowth, and furthermore address whether changes in the distribution of the Kv3.1b channel throughout the B35 cell could be attributed to differences in outward currents. In the earlier study, all four Kv3.1b proteins were tagged with FLAG epitope while for the current study proteins were fused to EGFP. The latter tag provided a means to evaluate spatial arrangement of Kv3.1b proteins in live B35 cells. To verify that the larger tag did not disrupt  $N$ -glycosylation processing of the Kv3.1b proteins, we examined  $N$ -glycosylation occupancy and  $N$ -glycan type. Total membranes were isolated from B35 cells expressing wild type, N220Q/N229Q, N220Q, or N229Q Kv3.1b proteins. These membranes were treated without (–) and with (+) PNGase F (removes complex, hybrid, and oligomannose  $N$ -glycans), neuraminidase (cleaves sialyl residues from non-reducing termini of carbohydrate chains), or Endo H (removes oligomannose and some hybrid  $N$ -glycans), and then analyzed by Western blotting. A major immunoband was observed for wild type ( $\approx 138$  kDa) (a), N220Q/N229Q ( $\approx 104$  kDa) (a), N220Q ( $\approx 120$  kDa) (b) and N229Q ( $\approx 120$  kDa) (b) Kv3.1b proteins (Fig. 1). The electrophoretic migrations were slowest for wild type and fastest for the aglycoform while that of the single glycosylation mutants were intermediate. Major bands for wild type, N220Q, and N229Q Kv3.1b proteins were sensitive to both PNGase F and neuraminidase treatment while they were resistant to Endo H treatment. Further the electrophoretic migrations were greater for the Kv3.1b glycoproteins treated with PNGase F than neuraminidase. The N220Q/N229Q Kv3.1b protein was resistant to all of the different

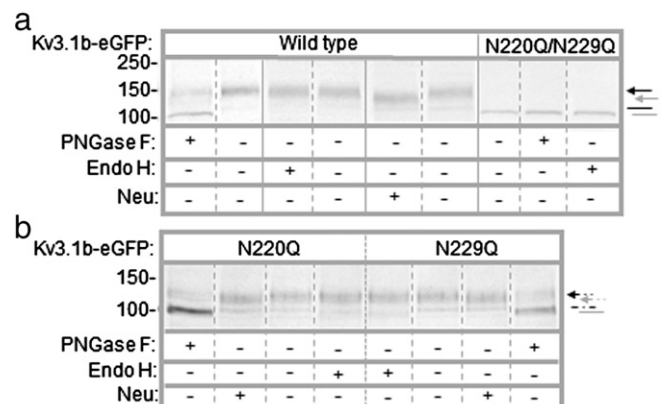


**Fig. 1.** The characterization of various forms of the Kv3.1b protein in B35 neuroblastoma cells by Western blotting. Blots of wild type (a), N220Q/N229Q (a), N220Q (cb), and N229Q (db) Kv3.1b proteins digested (+) and undigested (–) with PNGase F, Endo H, and neuraminidase (neu) when heterologously expressed in B35 neuroblastoma cells. Vertical solid gray lines indicate cut or separate blot. The numbers adjacent to the Western blots represent the Kaleidoscope markers (in kDa). Arrows in black or gray denote sialylated or asialylated complex  $N$ -glycan(s) of the Kv3.1b glycoprotein, while the black and gray solid lines represent oligomannose  $N$ -glycan(s) of the Kv3.1b glycoprotein and the unglycosylated Kv3.1b protein, respectively.



glycosidase treatments and the electrophoretic migration was similar to that of all three forms of the Kv3.1b glycoprotein treated with PNGase F. In some cases, a faint immunoband which migrated faster than the major band could be detected for wild type, N220Q or N229Q Kv3.1b proteins. In all cases, these faint immunobands were sensitive to PNGase F and Endo H while they were resistant to neuraminidase. Previously, it was shown that very small amounts of the various Kv3.1 glycoproteins escaped *cis*-Golgi processing [11]. Taken together, these results verified that two, one, one, and zero sialylated complex *N*-glycans could be attached to wild type (glycosylated), N220Q (partially glycosylated), N229Q (partially glycosylated), and N220Q/N229Q (unglycosylated) Kv3.1b proteins, respectively, and importantly that the EGFP tag did not disrupt protein folding.

### 3.2. Glycosylation impacts subcellular localization of the Kv3.1b protein

We utilized TIRF microscopy to ascertain whether *N*-glycosylation occupancy of Kv3.1b alters cell body and outgrowth localization of Kv3.1b in B35 neuroblastoma cells. High contrast images of wild type (a), N220Q/N229Q (b), N220Q (c) and N229Q (d) Kv3.1b proteins tagged with EGFP at the adherent membrane of live B35 neuroblastoma cells were acquired by TIRF microscopy (Fig. 2, top rows). Then, DIC images (Fig. 2, middle rows) were obtained in the same plane to designate the clusters of fluorescence signal to specific positions of the cell in TIRF images. Lastly, images were obtained from the same cell after changing the laser beam to achieve wide-field fluorescence excitation (Fig. 2, bottom rows). We found that the fluorescence intensity signals from TIRF images were of higher intensity than those from the wide-field images, with respect to both the entire cell (ratios of mean fluorescence intensity values of TIRF images to mean fluorescence intensity values of wide-field images were  $1.18 \pm 0.01$ ,  $n = 46$  and  $1.27 \pm 0.02$ ,  $n = 48$  for B35 cells expressing glycosylated and unglycosylated Kv3.1b, respectively) and cell body (ratios of mean fluorescence intensity values of TIRF images to mean fluorescence intensity values of wide-field images were  $1.27 \pm 0.01$ ,  $n = 46$  and  $1.28 \pm 0.02$ ,  $n = 48$  for B35 cells expressing glycosylated and unglycosylated Kv3.1b, respectively). The high signal to noise ratio supports that detailed spatial arrangement of Kv3.1b proteins at adherent plasma membrane could be obtained in the TIRF mode. Of note, the lower mean intensity ratio of entire cell relative to that of cell body determined for cells expressing glycosylated Kv3.1b protein was due to the amount of glycosylated Kv3.1b protein expressed in the thin outgrowths. Further the high values for the unglycosylated Kv3.1b protein verified that this mutant was trafficked to the plasma membrane, like the glycosylated Kv3.1b protein.

Cells expressing either the glycosylated or unglycosylated Kv3.1b proteins had a similar number of particles of comparable size per cell while those expressing either N220Q or N229Q Kv3.1b proteins had fewer particles per cell, but with larger particle size (Fig. 2e and f). However, the total area of fluorescence signal per cell for N220Q or N229Q Kv3.1b proteins transfected cells was 95% and 87% of wild type Kv3.1b transfected cells, respectively while that of N220Q/N229Q Kv3.1b protein transfected cells was 68%. The mean intensity was greater for cells expressing wild type and N229Q Kv3.1b proteins than those expressing N220Q/N229Q or N220Q (Fig. 2g). However, these differences in the mean intensity values did not alter the overall protein expression levels determined from the total fluorescence signal area of the unglycosylated and partially glycosylated Kv3.1b proteins relative to that of the fully glycosylated Kv3.1b protein. Taken together, these results suggest that quite similar amounts of glycosylated, unglycosylated, and partially glycosylated Kv3.1b proteins were expressed at the adherent plasma membrane but the density of Kv3.1b protein per particle for wild type and N229Q Kv3.1b proteins were higher than those of N220Q/N229Q and N220Q Kv3.1b proteins.

Fluorescence intensity signals were quite strong for cells expressing various forms of the Kv3.1b protein, and they could be observed in the outgrowths and cell body of cells. Although the mean particle number

was quite similar between these domains for cells expressing glycosylated Kv3.1b protein, there were more particles concentrated in the cell body for cells expressing unglycosylated and partially glycosylated Kv3.1b proteins (Fig. 2h). Ratios of mean particle number in cell body to that in outgrowth were 1.1, 1.7, 1.6, and 1.6 for cells expressing wild type, N220Q/N229Q, N220Q and N229Q Kv3.1b proteins, respectively. TIRF image analysis also revealed that the mean particle size for cells expressing N220Q/N229Q and N220Q Kv3.1b proteins was larger in the cell body than outgrowth while they were not significantly different for cells expressing wild type and N229Q Kv3.1b proteins (Fig. 2i). Ratios of mean particle sizes in the cell body to that in the outgrowth were 1.2, 7.3, 2.7 and 1.6 for cells expressing wild type, N220Q/N229Q, N220Q and N229Q Kv3.1b proteins, respectively. Ratios of the total area of fluorescence signal in cell body to that in outgrowth were about 1 for wild type, 2 for N229Q, 4 for N220Q and 12 for N220Q/N229Q Kv3.1b proteins. In all cases, mean fluorescence intensity of particles in cell body of the various cell lines was quite similar (Fig. 2j). Mean intensity values in the outgrowths were significantly higher than those in the cell body for cells expressing wild type and N229Q Kv3.1b proteins. Taken together, these results revealed that a similar amount of the fully glycosylated Kv3.1b protein was observed in both domains of neuroblastoma cells while the aglycoform had much more Kv3.1b protein in the cell body than in the outgrowth. Further the fully glycosylated and partially glycosylated N229Q Kv3.1b proteins formed higher density particles in the outgrowths than cell body. Both of the partially glycosylated Kv3.1b proteins favored localization in the cell body but to a lesser extent than the aglycoform. Additionally, the N220Q Kv3.1b protein had a higher preference for the cell body than the N229Q Kv3.1b protein.

### 3.3. Cell–Cell adhesion is enhanced by *N*-glycosylation of the Kv3.1 protein

Since *N*-glycans altered subcellular localization of the Kv3.1b protein in B35 cells, we evaluated whether these unique distribution patterns influenced the strength of cell–cell adhesion. Representative images of cell aggregates remaining after dissociation of a cell monolayer for transfected B35 cells with glycosylated (Fig. 3a), unglycosylated (Fig. 3b) Kv3.1b proteins, and nontransfected B35 cells (Fig. 3c). Analysis of these images revealed that the mean particle size of the cell aggregates (>2 cells/aggregate) was about 1.7-fold and 1.3-fold greater for the glycosylated and unglycosylated Kv3.1b than the nontransfected cells (Fig. 3d). Further cells expressing the glycosylated Kv3.1b protein had cell aggregates about 1.4-fold larger than those expressing the unglycosylated Kv3.1 protein. Cells transfected with either wild type or N220Q/N229Q Kv3.1b proteins had approximately 1.6-fold greater percent of large cell aggregates (>5 cells/aggregate) than the nontransfected cells (Fig. 3e). Conversely, the nontransfected cells resulted in a greater percent of small aggregates (2–5 cells/aggregate) than those observed for the glycosylated or unglycosylated Kv3.1b proteins. In short, these results revealed the ability of B35 cells expressing the glycosylated Kv3.1b protein to resist aggregate disruption to a greater extent than those expressing its unglycosylated counterpart, and even greater than the nontransfected cells. As such, expression of the Kv3.1b protein in B35 cells results in strengthening adhesive contacts between neighboring cells, and furthermore attachment of the *N*-glycans to the Kv3.1b protein enhances the strength of cell–cell adhesion.

### 3.4. Cell–cell association is influenced by the glycosylation of the Kv3.1 protein

Since expression and distribution of the Kv3.1b protein throughout the adherent plasma membrane influenced cell–cell adhesion, it was addressed whether cells transfected with the Kv3.1b protein affected cell aggregate formation in cell suspensions. Representative images of cell–cell association in the presence of calcium at 40 min are shown for cells expressing glycosylated (Fig. 4a) and unglycosylated (Fig. 4b)

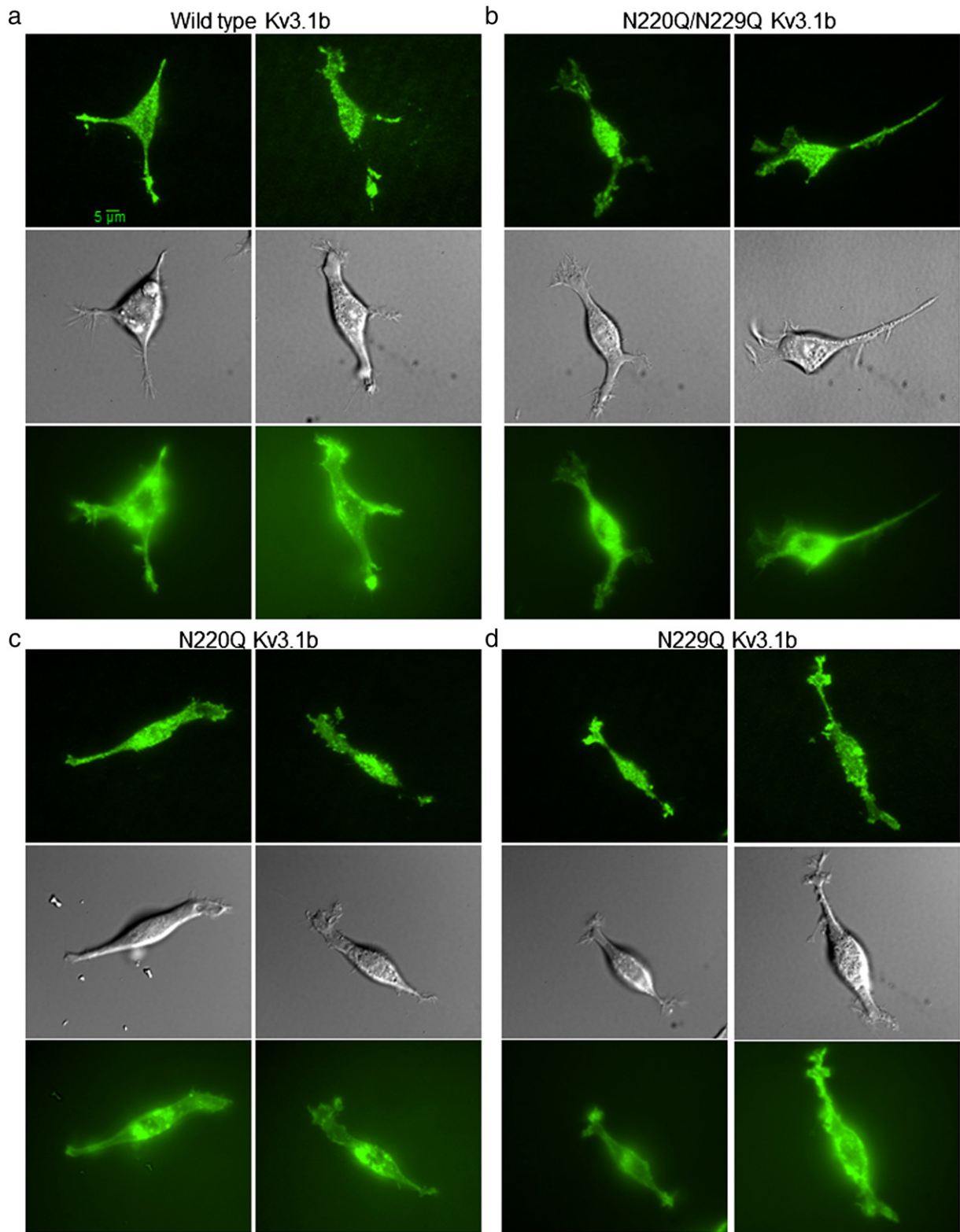


**Fig. 2.** Microscopy images were acquired in TIRF (upper panels), DIC (middle panels), and wide-field (lower panels) modes for EGFP tagged wild type (a), N220Q/N229Q (b), N220Q (c), and N229Q (d) Kv3.1b proteins expressed in B35 neuroblastoma cells. Representative scale bar (5  $\mu\text{m}$ ) was identical for all images. The number of fluorescence particles (e), average size of those particles (f), and the mean intensity (g) was determined for the entire cell. Particle number (h), particle size (i), and mean intensity (j) were also determined for cell body (CB) and outgrowth (OG). Data are presented as the mean  $\pm$  S.E. and  $n$  denotes the number of cells (e, f & g), cell bodies, and outgrowths. The number of cell bodies was similar to the number of cells while the number of outgrowths was 112, 114, 80 and 95 for wild type, N220Q/N229Q, N220Q, and N229Q, respectively (h). The number of cell bodies with particles was 39, 46, 33 and 38 and the number of outgrowths with particles was 111, 107, 75 and 93 for wild type, N220Q/N229Q, N220Q, and N229Q, respectively, (i & j). Data are presented as the mean  $\pm$  S.E. Mean differences were compared by student's  $t$  test. Asterisks (\*) indicate significant differences in mean values relative to wild type Kv3.1b transfected cells (e, f & g) and those between the cell body and outgrowth (h, i & j) at a probability of 0.05. NS denotes the mean values were not significantly different.

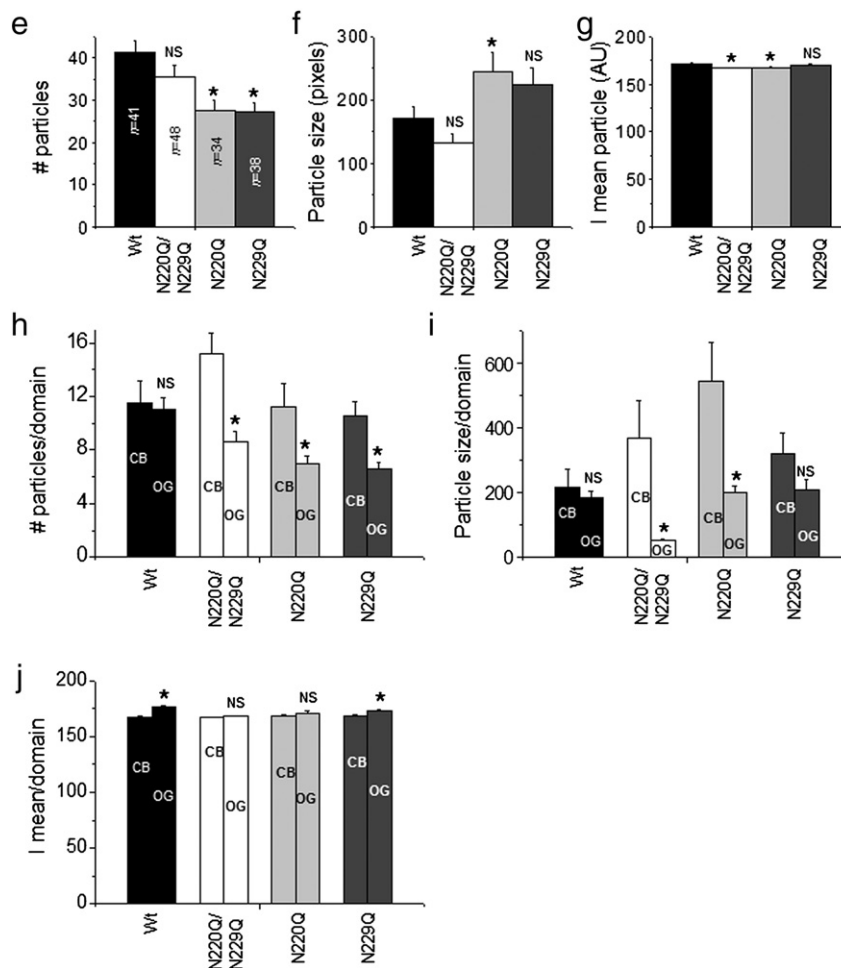


Fig. 2. (continued).

Kv3.1b proteins, along with nontransfected cells (Fig. 4c). These images revealed that aggregates formed from cells expressing the Kv3.1b glycoprotein were smaller than those expressing unglycosylated Kv3.1b, and much smaller than the nontransfected cell aggregates. The mean particle size of cell aggregates expressing glycosylated Kv3.1b was about 1.7-fold smaller than that from cells expressing unglycosylated Kv3.1b and it was about 5.9-fold smaller than nontransfected cells (Fig. 4d). Aggregates of cells expressing unglycosylated Kv3.1b were about 3.3-fold smaller than aggregates of nontransfected cells. In all cases, the mean particle size in the presence of calcium at 0 min was  $1071 \pm 184$  pixels,  $n = 55$ ;  $1901 \pm 950$  pixels,  $n = 44$ ;  $832 \pm 245$  pixels,  $n = 56$  for wild type and N220Q/N229Q Kv3.1b transfected and nontransfected B35 cells, respectively. The values of the mean particle size in the absence of calcium at these same time points were not significantly different from the 0 min time point with calcium. Thus, these results indicate that the Kv3.1b protein decreases the ability of the cells to associate in a calcium-dependent manner, and furthermore glycans attached to the Kv3.1b glycoprotein further decrease cell association.

To elaborate on the impact of the Kv3.1b protein on cell aggregation, the hanging drop assay was conducted. Representative images of aggregates formed after 24h incubation in the hanging drop for cells expressing glycosylated (Fig. 5a), unglycosylated (Fig. 5b) Kv3.1b proteins, and nontransfected cells (Fig. 5c). The mean particle size of cells transfected with wild type Kv3.1b protein was smaller than that of cells transfected with N220Q/N229Q and much smaller than that of nontransfected cells (Fig. 5d). Notable differences in the morphology of the aggregates formed were observed. Compact spheroids consisting of cells smaller in size (Fig. 5e, upper), along with the loosely organized aggregates

with larger cells (Fig. 5e, lower), were noted. Both types of aggregates were represented in all three cell populations but the loosely organized aggregates formed by far the majority of the aggregates. Wild type Kv3.1b cells displayed a greater percentage of fields with compact spherical aggregates than the unglycosylated Kv3.1b cells and much greater than the nontransfected cell population (Fig. 5f). Both loose sheet-like aggregates and compact spheroids for various cancer cells using this same technique have previously been reported [18]. These results verify the classical aggregation assay results, and furthermore indicate that the Kv3.1b glycoprotein contributes to the compaction of the aggregates.

#### 4. Discussion

For the present study, we have utilized rat B35 neuroblastoma cells to investigate effects of N-glycosylation on Kv3.1b protein clustering in the cell body and outgrowth domains of a neuron-like cell, along with cell adhesion properties. B35 neuroblastoma cells provide a standard cellular model for the investigation of neuronal-like cellular properties [17]. Recently, we have shown that heterologous expression of the Kv3.1b protein, including wild type, N220Q, N229Q, and N220Q/N229Q Kv3.1b proteins, in B35 cells enhances cell migration, and furthermore that the number of occupied N-glycosylation sites of the Kv3.1b protein also had an impact on the rates of cellular migration [11]. Additionally, we showed that fully glycosylated, partially glycosylated, and unglycosylated Kv3.1b proteins preferred different whole cell current patterns, and the Kv3.1b channels had different opening and closing rates. In the current study, we provide insight into how the



various forms of the Kv3.1b protein impact its spatial arrangement, including the degree of Kv3.1b protein clustering, in the cell body and outgrowth domains of B35 cells, and in turn alter cell migration, cell adhesion and ion conductance properties. Using TIRF microscopic analysis of GFP tagged Kv3.1b proteins, we found that the fully glycosylated Kv3.1b protein localized equally well to both the cell body and outgrowth, while unglycosylated and partially glycosylated Kv3.1b proteins preferentially localized to the cell body. Higher density Kv3.1b particles were also observed in the outgrowth as compared to the cell body for both the fully glycosylated Kv3.1b protein and the partially glycosylated N229Q Kv3.1b protein while this was not the case for neither the aglycoform nor the other partially glycosylated N220Q Kv3.1b protein.

Naturally occupied *N*-glycosylation sites of glycoproteins may influence many of their properties which include folding, stability, solubility, antigenicity clearance rate, degradation, and in vivo activity [2]. Our results would suggest that synthesis and degradation rates were similar for all four forms of the Kv3.1b protein since their protein levels were quite comparable in the B35 cells. Further the level of the fully glycosylated and unglycosylated Kv3.1b channels at the cell surface were remarkably identical as determined from the maximum current amplitude divided by the cell capacitance [19]. On the contrary, the density of the Kv3.1b molecules per particle, also referred to as a Kv3.1b protein cluster, was greater for the fully glycosylated and partially glycosylated N229Q Kv3.1b protein than those of the partially glycosylated N220Q and unglycosylated Kv3.1b proteins. The number and position of glycans contributed to the density of the Kv3.1b particles, indicating that the glycans are participating in glycoprotein–glycoprotein interaction of these high

density particles. Previous studies have shown that carbohydrate-to-carbohydrate interactions participate in membrane organization [20]. Changes in the stability of tertiary structure and/or quaternary structure of the various forms of the Kv3.1b protein could also be adding to the differences in particle density. Alternatively, it may be that enrichment of the glycoprotein per particle occurs due to crosslinking of the fully and partially glycosylated Kv3.1b proteins to galectins [4]. Nonetheless, our data, including the expression of fully glycosylated Kv3.1b throughout the central nervous system [8], support that if *N*-glycan attachment would be aberrant, such as in humans suffering from CDG [14], then the spatial arrangement of Kv3.1b proteins, lacking one or two *N*-linked glycans, would be different from that of the fully glycosylated Kv3.1b protein, and furthermore the Kv3.1b protein clusters would be less dense for the partially glycosylated N220Q and unglycosylated Kv3.1b proteins in the outgrowths.

Neuronal polarity has been broadly described as segregation of various protein and lipid collections to axonal and somatodendritic domains [21]. In some cases, distinct sets of membrane proteins are specific for a particular cellular domain. In other cases, the same protein may reside in both domains but at different protein levels. The latter condition has been described for the localization of both Kv3.1 splice variant proteins [10]. For instance, Kv3.1a was quite limited to the axonal processes of the mammalian brain while Kv3.1b was well distributed between the neuronal somata and processes [22]. Here we observed that when both *N*-glycans were attached to the Kv3.1b protein, the number and size of the Kv3.1b protein particles were quite similar in the cell body and outgrowth. However, the number of Kv3.1b glycoprotein molecules per particle was higher in the outgrowth than cell body. When *N*-glycosylation sites were not occupied at positions 220 and 229 of the Kv3.1b protein, the number and size of Kv3.1b protein particles were greater in the cell body than the outgrowth. Further the

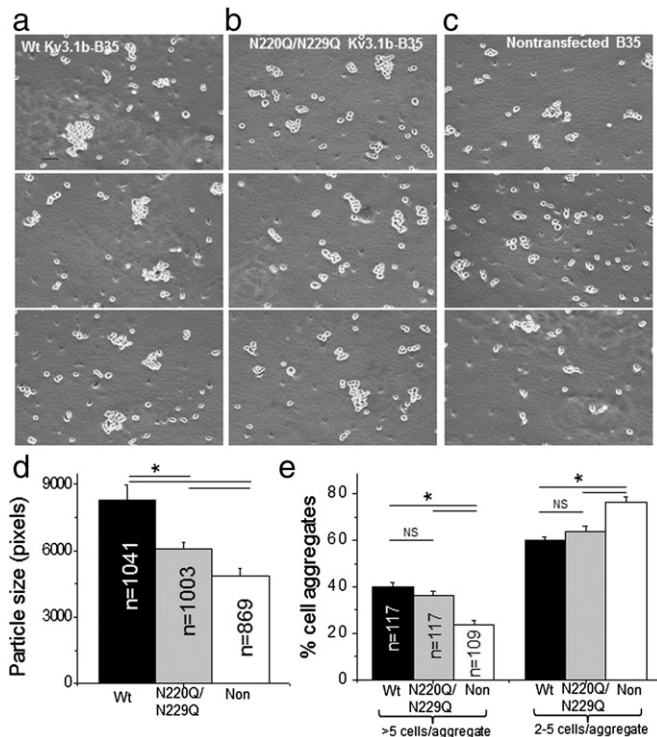


**Fig. 3.** Kv3.1b alters dissociation of cell aggregates. Cell adhesion of Kv3.1b transfected B35 cells was evaluated by the cell dissociation assay. Microscopy images were acquired for wild type (a) and N220Q/N229Q (b) Kv3.1b transfected cells, and nontransfected cells (c). Particle sizes were analyzed for cell aggregates with  $\geq 2$  cells (d). The scale bar denotes 129 pixels or 0.25  $\mu\text{m}$ . The percent of cell aggregates was calculated for particles comprised of  $>5$  cells (left), and for particles with 2–5 cells (right) (e). Data are presented as the mean  $\pm$  S.E. and *n* denotes the number of particles (d) and images (e). Mean differences were compared by student's *t* test. Asterisks indicate significant differences in mean values at a probability of 0.05 and NS signifies that the mean values were not significantly different.

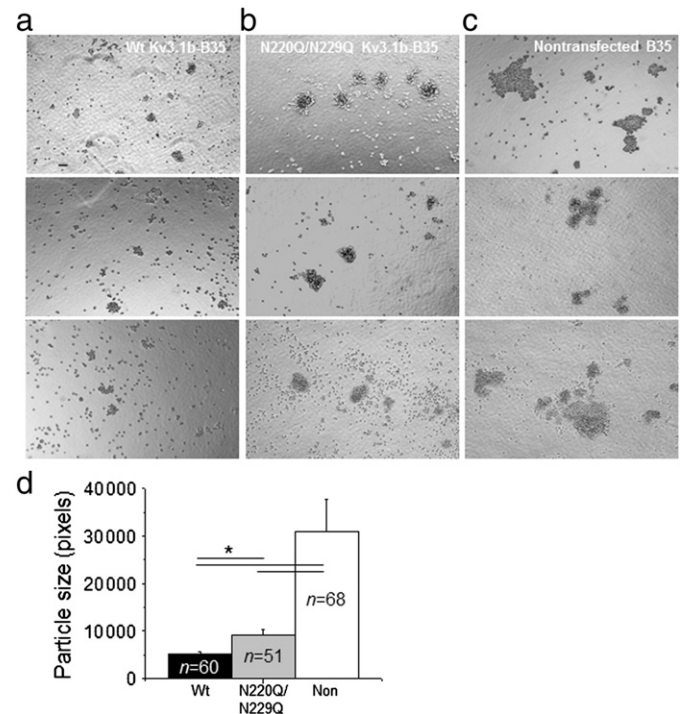


**Fig. 4.** Kv3.1b influences cell–cell association in the presence of calcium. The classical cell association assay was employed to compare cell aggregation of nontransfected B35 cells to Kv3.1b transfected B35 cells. Microscopy images were acquired for wild type (a) and N220Q/N229Q (b) Kv3.1b expressing cells, as well as nontransfected cells (c). The scale bar represents 64 pixels or 0.25  $\mu\text{m}$ . Particle sizes were determined for cell aggregates composed of  $>10$  cells (d). Each bar represents mean numbers  $\pm$  S.E., and *n* denotes the number of particles. Asterisks denote significant differences in mean values at a probability of 0.05.

density of the Kv3.1b protein per particle was similar in both domains or similar to that of the fully glycosylated Kv3.1b in the cell body. When either one of the sites was not occupied, then the number of Kv3.1b protein particles favored localization to the cell body, like the aglycoform. The N220Q Kv3.1b protein was also like the aglycoform in that larger Kv3.1b particles were observed in the cell body than outgrowths, and the density of the Kv3.1b protein per particle was similar in both domains. On the contrary, the N229Q Kv3.1b protein was more similar to the fully glycosylated Kv3.1b protein since sizes of the Kv3.1b particles were quite similar between the cell body and outgrowth, and furthermore the density of the Kv3.1b protein per particle was greater in the outgrowth than the cell body. Taken together, our study reveals that *N*-glycans of the Kv3.1 protein contain information on its lateral heterogeneity in the cell membrane. As such, segregation of glycans, like proteins and lipids, contribute to neuronal polarity.

Since the *N*-glycans of Kv3.1b contributed to its segregation in the membrane of the cell body and outgrowths of neuronal-derived cells, glycans of other glycosylated membrane proteins would most likely provide information for them as well. Further the distributions of glycosylated Kv channels in neurons of mammalian brain would be influenced by normal or abnormal *N*-glycosylation processing. For instance, Kv3.1a protein was much more strongly localized to the axonal processes of mammalian brain than Kv3.1b [22]. As such, it would be expected that in B35 cells the fully glycosylated form of the Kv3.1a would be more

localized to the outgrowths than cell body. Further if *N*-glycosylation sites were unoccupied then more of the Kv3.1a protein would be expected to localize to the cell body of B35 cells, or less Kv3.1a protein distributed to axonal processes of mammalian brain. Another notable feature is that high density clusters of the Kv3.1b channel were reported in the node of Ranvier of mammalian axons [10] which correlates with the higher density Kv3.1b particles in the outgrowth compared to the cell body in B35 cells. A more recent study has revealed that various glycan structures associated with Kv3.1b, as well as E-cadherin, had an impact on their topographical arrangements in the cell membrane [23] which supports the importance of *N*-glycans in organization of glycosylated transmembrane proteins in neurons of mammalian brain. Taken together, our results indicate that the segregation and clustering of the Kv3.1b glycoprotein, as well as other Kv channels in neuronal membranes are strongly influenced by the number and position of its *N*-glycans.

Previously, we have shown that the number and position of the *N*-glycans associated with the Kv3.1b channel favored distinct whole cell current patterns [11]. Both the fully glycosylated and partially glycosylated N229Q Kv3.1b channels preferred noninactivating currents while the partially glycosylated N220Q and unglycosylated N220Q/N229Q Kv3.1b channels favored the inactivating current type. The noninactivating current type represents current amplitudes that lack saturation at more depolarized potentials, and these currents usually have transient peaks

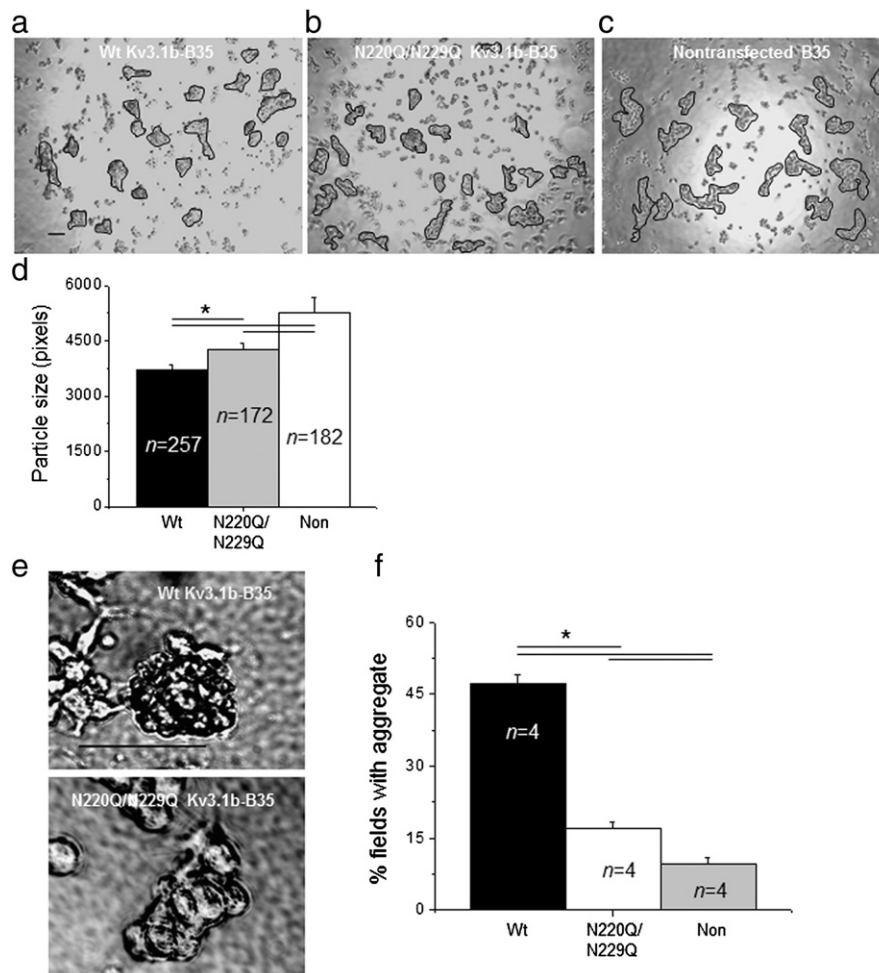


**Fig. 5.** Kv3.1b alters formation of cell aggregates. Cell–cell association of Kv3.1b transfected B35 cells and nontransfected B35 cells was evaluated using the hanging drop assay. Microscopy images were acquired for wild type (a) and N220Q/N229Q (b) Kv3.1b transfected cells, along with nontransfected cells (c). Encircled areas denote particles (> cells/aggregate) measured. The scale bar indicates 64 pixels or 0.25  $\mu$ m (a) and 264 pixels or 0.25  $\mu$ m (e), respectively. The average particle size was determined for each cell type (d). Representative images of a tight aggregate (upper) and a loose aggregate (lower) are displayed (e). The percent of fields containing at least one tight aggregate was calculated (f). Data are presented as the mean number  $\pm$  S.E. and *n* denotes the number of particles (d) and experiments (f). Asterisks signify significant differences in mean values at a probability of 0.05.



[24–26]. The inactivating current type represents saturation of current amplitudes at more depolarized potentials [27]. Interestingly, these preferential current types expressed by the various forms of the Kv3.1b channel can be explained by their topographical arrangements in the cell membrane. Both the fully glycosylated and partially glycosylated N229Q Kv3.1b channels expressed a higher density of Kv3.1b molecules per particle in the outgrowth than the unglycosylated and partially glycosylated N220Q Kv3.1b channels. As such, the outward ionic currents expressed by the earlier two forms of the Kv3.1b channel were more likely to lack saturation at greater depolarized potentials. Another interesting point is that the fully and partially glycosylated Kv3.1b channels had a preference for the noninactivating current type with transient peaks while the unglycosylated Kv3.1b channel favored this current type without transient peaks. This current preference of the fully and partially glycosylated Kv3.1 channels may be explained by larger amounts of the Kv3.1b protein in the outgrowths relative to that of the unglycosylated Kv3.1b protein. Thirdly, opening and closing rates of the Kv3.1b channel were greatly reduced by the vacancy of both *N*-glycosylation sites for either current type while they were solely decreased for the inactivating current type when one of the sites was vacant. We attribute these differences in the rates to the much lower level of the unglycosylated Kv3.1b protein, as well as the lower level of partially glycosylated Kv3.1b proteins, in the outgrowth to cell body compared to the fully glycosylated Kv3.1b channel. Another study has shown that Kv3.1 splice variants in cultured hippocampal neurons were unequally distributed in the plasma membrane, and furthermore their dissimilarities in distribution modified the firing frequency of neurons [28]. Taken together, these studies support that *N*-glycosylation site occupancy and position of the Kv3.1b protein can achieve different orchestrated patterns of electrical activity by localizing different levels of Kv3.1b channels to specific regions in the plasma membrane of neuronal cells. Further it would be of importance to determine how *N*-glycosylation processing of Kv3.1 splice variants impact spiking frequency of neuronal cells.

An important issue raised by our findings is that changes in cellular properties can be supported by the different distributions of various glycosylated forms of the Kv3.1b protein in the B35 cells. Previously, we showed that cell migratory rates were slowest for the unglycosylated Kv3.1b protein, fastest for the fully glycosylated Kv3.1b protein, and intermediate for partially glycosylated Kv3.1b proteins [11]. Since more Kv3.1b protein was expressed in outgrowths for the fully glycosylated Kv3.1b protein than either of the partially glycosylated Kv3.1b proteins, and much more than that of the aglycoform, the results support that the localization of the Kv3.1b protein to outgrowths contributes to the migratory rates of the B35 cells. Strength of cell–cell interactions also appeared to be enhanced by greater amounts of the Kv3.1b protein in the outgrowths since dissociated cell monolayers produced larger cell aggregates for the fully glycosylated Kv3.1b protein than the aglycoform. Additionally, B35 cells in cell suspension cultures expressing the fully glycosylated Kv3.1b protein formed more compact spheroidal cell aggregates than cells expressing the Kv3.1b aglycoform. Alternatively, loose cell aggregates of smaller size were detected for the fully glycosylated Kv3.1b protein than the aglycoform. Of note, the dissociation assay measures the disruption of cell aggregates in a monolayer while the hanging drop assay, like the classical association assay, reports the ability of the cells in suspension to aggregate. As such, it may be that when monolayers are formed the outgrowths are the major contributors to the tight cell–cell adhesion, and furthermore that the glycosylated Kv3.1 has more protein in outgrowths. In contrast, when the association of cells was measured, the cell body is most likely the major contributor to the size of the cell aggregates since outgrowths tend to retract when cells are in suspension cultures. Further when the cells attach and aggregate, as in the hanging drop assay, the compact spheroidal cell aggregates may form due to greater extension of the outgrowths. Therefore, the number and placement of *N*-glycans associated with the Kv3.1b protein enhance the cellular migratory rates, the strength of cell–cell adhesion, and compaction of cell aggregates. Since

these cellular properties involve numerous proteins, our results suggest that the different distributions of the various forms of the Kv3.1b glycoprotein could directly and indirectly modify their biological roles which in turn impact cell adhesion and migration properties.

## 5. Conclusion

We conclude that the level and location of *N*-linked glycan site occupancy for the Kv3.1b protein are a critical determinant in the distribution of this protein between the cell body and outgrowth of B35 cells. The fully glycosylated Kv3.1b protein had a higher distribution in outgrowths of a neuronal-derived cell than that of the partially glycosylated N229Q Kv3.1b protein, followed closely by that of the partially N220Q Kv3.1b protein, and much higher than that of the aglycoform. Further both the fully glycosylated and partially glycosylated N229Q Kv3.1b proteins formed higher density particles in the outgrowth than cell body. Our current study, along with our previous study [11], demonstrated the functional significance of the Kv3.1b protein distribution in cell outgrowths as measured by increased strength of cell–cell interaction, enhanced cell migratory rates and preference for noninactivating currents with transient peaks, and increased activation and deactivation rates of ionic currents. Taken together, these results suggest that the glycan content of Kv3.1b membrane proteins contains information that guides their spatial arrangement in the cell membrane, and thus influences their cellular function.

## Acknowledgements

None.

## References

- [1] R. Apweiler, H. Hermjakob, N. Sharon, On the frequency of protein glycosylation, as deduced from analysis of the SWISS-PROT database, *Biochim. Biophys. Acta* 1473 (1999) 4–8.
- [2] J. Jones, S.S. Krag, M.J. Betenbaugh, Controlling *N*-linked glycan site occupancy, *Biochim. Biophys. Acta* 1726 (2005) 121–137.
- [3] O. Vagin, J.A. Kraut, G. Sachs, Role of *N*-glycosylation in trafficking of apical membrane proteins in epithelia, *Am. J. Physiol. Renal. Physiol.* 296 (2009) F459–F469.
- [4] K.S. Lau, E.A. Partridge, A. Grigorian, C.I. Silvescu, V.N. Reinhold, M. Demetriou, J.W. Dennis, Complex *N*-glycan number and degree of branching cooperate to regulate cell proliferation and differentiation, *Cell* 129 (2007) 123–134.
- [5] B. Hille, *Ionic Channels of Excitable Membranes*, 3rd ed. Sinauer, Sunderland, MA, 2001.
- [6] L.K. Kaczmarek, Non-conducting functions of voltage-gated ion channels, *Nat. Rev. Neurosci.* 7 (2006) 761–771.
- [7] T.A. Cartwright, M.J. Corey, R.A. Schwalbe, Complex oligosaccharides are *N*-linked to Kv3 voltage-gated K<sup>+</sup> channels in rat brain, *Biochim. Biophys. Acta* 1770 (2007) 666–671.
- [8] R.A. Schwalbe, M.J. Corey, T.A. Cartwright, Novel Kv3 glycoforms differentially expressed in adult mammalian brain contain sialylated *N*-glycans, *Biochem. Cell Biol.* 86 (2008) 21–30.
- [9] C.J. Luneau, J.B. Williams, J. Marshall, E.S. Levitan, C. Oliva, J.S. Smith, J. Antanavage, K. Folander, R.B. Stein, R. Swanson, et al., Alternative splicing contributes to K<sup>+</sup> channel diversity in the mammalian central nervous system, *Proc. Natl. Acad. Sci. U. S. A.* 88 (1991) 3932–3936.
- [10] H. Vacher, D.P. Mohapatra, J.S. Trimmer, Localization and targeting of voltage-dependent ion channels in mammalian central neurons, *Physiol. Rev.* 88 (2008) 1407–1447.
- [11] M.K. Hall, T.A. Cartwright, C.M. Fleming, R.A. Schwalbe, Importance of glycosylation on function of a potassium channel in neuroblastoma cells, *PLoS One* 6 (2011) e19317.
- [12] M.K. Hall, W. Reutter, T. Lindhorst, R.A. Schwalbe, Biochemical engineering of the *N*-acyl side chain of sialic acids alters the kinetics of a glycosylated potassium channel Kv3.1, *FEBS Lett.* 585 (2011) 3322–3327.
- [13] A.R. Ednie, E.S. Bennett, Modulation of voltage-gated ion channels by sialylation, *Compr. Physiol.* 2 (2012) 1269–1301.
- [14] J. Jaeken, Congenital disorders of glycosylation, *Ann. N. Y. Acad. Sci.* 1214 (2010) 190–198.
- [15] M.F. Waters, N.A. Minasian, G. Stevanin, K.P. Figueroa, J.P. Bannister, D. Nolte, A.F. Mock, V.G. Evidente, D.B. Fee, U. Muller, A. Durr, A. Brice, D.M. Papazian, S.M. Pulst, Mutations in voltage-gated potassium channel KCNC3 cause degenerative and developmental central nervous system phenotypes, *Nat. Genet.* 38 (2006) 447–451.

- [16] J. Ousingsawat, M. Spitzner, S. Puntheeranurak, L. Terracciano, L. Tornillo, L. Bubendorf, K. Kunzelmann, R. Schreiber, Expression of voltage-gated potassium channels in human and mouse colonic carcinoma, *Clin. Cancer Res.* 13 (2007) 824–831.
- [17] C.A. Otey, M. Boukhelifa, P. Maness, B35 neuroblastoma cells: an easily transfected, cultured cell model of central nervous system neurons, *Methods Cell Biol.* 71 (2003) 287–304.
- [18] K.L. Sodek, M.J. Ringuette, T.J. Brown, Compact spheroid formation by ovarian cancer cells is associated with contractile behavior and an invasive phenotype, *Int. J. Cancer* 124 (2009) 2060–2070.
- [19] N.L. Brooks, M.J. Corey, R.A. Schwalbe, Characterization of N-glycosylation consensus sequences in the Kv3.1 channel, *Febs J.* 273 (2006) 3287–3300.
- [20] S. Hakomori, Carbohydrate-to-carbohydrate interaction, through glycosynapse, as a basis of cell recognition and membrane organization, *Glycoconj. J.* 21 (2004) 125–137.
- [21] A.C. Horton, M.D. Ehlers, Neuronal polarity and trafficking, *Neuron* 40 (2003) 277–295.
- [22] A. Ozaita, M.E. Martone, M.H. Ellisman, B. Rudy, Differential subcellular localization of the two alternatively spliced isoforms of the Kv3.1 potassium channel subunit in brain, *J. Neurophysiol.* 88 (2002) 394–408.
- [23] M.K. Hall, D.A. Weidner, J.M. Chen, C.J. Bernetski, R.A. Schwalbe, Glycan structures contain information for the spatial arrangement of glycoproteins in the plasma membrane, *PLoS One* 8 (2013) e75013.
- [24] S.D. Critz, B.A. Wible, H.S. Lopez, A.M. Brown, Stable expression and regulation of a rat brain K<sup>+</sup> channel, *J. Neurochem.* 60 (1993) 1175–1178.
- [25] T. Kanemasa, L. Gan, T.M. Perney, L.Y. Wang, L.K. Kaczmarek, Electrophysiological and pharmacological characterization of a mammalian Shaw channel expressed in NIH 3T3 fibroblasts, *J. Neurophysiol.* 74 (1995) 207–217.
- [26] C.M. Macica, C.A. von Hehn, L.Y. Wang, C.S. Ho, S. Yokoyama, R.H. Joho, L.K. Kaczmarek, Modulation of the kv3.1b potassium channel isoform adjusts the fidelity of the firing pattern of auditory neurons, *J. Neurosci.* 23 (2003) 1133–1141.
- [27] Y. Ito, S. Yokoyama, H. Higashida, Potassium channels cloned from neuroblastoma cells display slowly inactivating outward currents in *Xenopus* oocytes, *Proc. Biol. Sci.* 248 (1992) 95–101.
- [28] Y. Gu, J. Barry, R. McDougel, D. Terman, C. Gu, Alternative splicing regulates kv3.1 polarized targeting to adjust maximal spiking frequency, *J. Biol. Chem.* 287 (2012) 1755–1769.